Journal of
Composites Science

MDPI

Article

Enhancing Strength and Toughness of Aluminum Laminated Composites through Hybrid Reinforcement Using Dispersion Engineering

Behzad Sadeghi [1,*], Pasquale Cavaliere [1] and Behzad Sadeghian [2]

[1] Department of Innovation Engineering, University of Salento, Via per Arnesano, 73100 Lecce, Italy; pasquale.cavaliere@unisalento.it
[2] Department of Materials Engineering, Isfahan University of Technology, Isfahan 84156-83111, Iran; behzadsadeghian91@gmail.com
* Correspondence: b.sadeghi2020@gmail.com

Abstract: In this work, we propose a hybrid approach to solve the challenge of balancing strength and ductility in aluminum (Al) matrix composites. While some elements of our approach have been used in previous studies, such as in situ synthesis and ex situ augmentation, our work is innovative as it combines these techniques with specialized equipment to achieve success. We synthesized nanoscale Al_3BC particles in situ using ultra-fine particles by incorporating carbon nanotubes (CNTs) into elemental powder mixtures, followed by mechanical activation and annealing, to obtain granular (UFG) Al. The resulting in situ nanoscale Al_3BC particles are uniformly dispersed within the UFG Al particles, resulting in improved strength and strain hardening. By innovating the unique combination of nanoscale Al_3BC particles synthesized in situ in UFG Al, we enabled better integration with the matrix and a strong interface. This combination provides a balance of strength and flexibility, which represents a major breakthrough in the study of composites. (Al_3BC, CNT)/UFG Al composites exhibit simultaneous increases in strength (394 MPa) and total elongation (19.7%), indicating increased strength and suggesting that there are promising strengthening effects of in situ/ex situ reinforcement that benefit from the uniform dispersion and the strong interface with the matrix. Potential applications include lightweight and high-strength components for use in aerospace and automotive industries, as well as structural materials for use in advanced mechanical systems that require both high strength and toughness.

Keywords: laminated composites; aluminum matrix composite; nanoscale Al_3BC; CNT; in situ; dispersion engineering; strength; toughness

Citation: Sadeghi, B.; Cavaliere, P.; Sadeghian, B. Enhancing Strength and Toughness of Aluminum Laminated Composites through Hybrid Reinforcement Using Dispersion Engineering. *J. Compos. Sci.* **2023**, *7*, 332. https://doi.org/10.3390/jcs7080332

Academic Editor: Yuan Chen

Received: 31 July 2023
Revised: 11 August 2023
Accepted: 14 August 2023
Published: 16 August 2023

1. Introduction

Hybrid reinforcement is a novel and significant strategy, the core idea of which is the use of hybrid reinforcements to exert respective advantages and fabricate advanced MMCs that are currently motivated by the purpose of overcoming the strength–ductility trade-off [1–5]. Due to the higher efficiency of nano-sized reinforcements compared to the counterpart micron-sized reinforcements [6], a step forward has been taken in the pursuit of simultaneous improvement of strength and ductility. Although the use of ex situ non-reinforcement always brings the dilemma of uniform dispersion in MMCs [7,8]. Along with all of the advantages of using ex situ reinforcements, deleterious aspects, such as the formation of incoherent interfaces between the reinforcement-matrix, problems such as stress concentration and deformation discontinuity at the microscale scale during the deformation process emerge [9,10]. Therefore, it seems that the simultaneous use of the benefits of in situ and ex situ reinforcements as part of a hybrid reinforcement strategy would be one of the optimal ways to realize the simultaneous improvement of strength and ductility in MMCs.

Recently, the laminated structures that imitate the structure of nacre were noticeably succussed to provide materials that were both strong and damage tolerant [11,12]. Furthermore, a reinforcement strategy based on the core idea of using hybrid reinforcements to exert their respective advantages to achieve synergistic effects, leading to excellent overall performance, has been demonstrated [4,5]. In addition, the grain refinement of the matrix grains, which is apparently one of the best ways of simultaneously improving the strength–ductility relationship, could not overcome the dislocation annihilation at grain boundaries (GBs), which leads to fast exhaustion of the strain-hardening capacity [13]. To cope with this issue, by employing a graphene (GNS)–copper (Cu) hybrid material, exceptional tensile strength and ductility has been achieved using a heterogenous structure [14]. Creating a laminated structure accompanied by hybrid reinforcement significantly contributes to hetero-deformation-induced (HDI) stress strengthening and sustained strain hardening, generating the key mechanical properties of GNS-Cu/Al. Moreover, high-performance reinforcement and a tailored architecture has been gained using a reduced graphene oxide (RGO)–CNT hybrid/Al composite prepared through a composite flake assembly process due to the formation of a planar network of RGO and CNT, which improves the load transfer efficiency between the matrix and the reinforcement in composites [5]. Recently, a strong and tough AMC reinforcement with graphene oxide (GO)–CNT hybrid was prepared via powder metallurgy [4]. The strength of the composites was improved via the synergistic effect of carbon nanotubes using in situ Al_4C_3 and GO. More recently, superior tensile properties of AMC reinforced using both in situ Al_2O_3 nanoparticles and ex situ GNSs, which were developed by manipulating the PM route [15]. The composite possesses a high tensile strength of 464 MPa and appreciable amount of ductility (8.9%), which result from the combination effect of grain refinement, in situ Al_2O_3 nanoparticles, and ex situ GNSs. It was inferred that the presence of a synergetic strategy between in situ and ex situ reinforcements, accompanied by a tailored architecture, could provide a significant contribution to both strengthening and toughening mechanisms to achieve the best combination of strength and ductility. Promisingly, the configuration of a microstructure in mesoscale and uniform spatial distribution of hybrid reinforcements offers great potential regarding the tuning of the mechanical properties of advanced AMCs [16]. Motivated by the above considerations, an easy and innovative route on the basis of elemental powder strategy via in situ synthesis was employed to introduce nano-Al_3BC into Al matrix composite reinforced with CNTs to attain a significant synergy of high strength and toughness. This method differs from those used by other researchers in several ways: 1—High-speed cutting and coating: High-speed cutting is used to break the CNT group, and B is used as a new step in manufacturing. This step allows carbon nanotubes to be dispersed within the Al matrix, which can improve the mechanical properties. 2—Micro–micro rolling (MMR) process: The MMR process involves micro-scale rolling of composite materials and appears to be a unique and innovative process used in the production of laminated composites. This process will introduce microstructures and textures that can help improve the properties of (Al_3BC, CNT)/Al composites. 3—In Situ Formation of Al_3BC: The in situ formation of Al_3BC particles in composites through the reaction of Al particles with B and carbon elements and subsequent annealing distinguishes this method from another method based on the addition of preformed particles. This in situ synthesis provides better control of the size, distribution, and coupling between the material and the matrix. 4—Low growth of Al_3BC: This method relies on using a solid-state reaction to produce low-growth Al_3BC particles, resulting in nanoscale Al_3BC particles with unique properties being produced. The presence of Al_4C_3 can also assist in the formation of submicron-sized heterogeneous core layers, such as Al_3BC particles. 5—Minimal damage to CNTs: Experiments show that CNTs suffer little or no major damage during pre-dispersion, extrusion, and MMR, which suggests that a careful and well-optimized approach is used to preserve the integrity of CNTs in composites. We demonstrated that a synergetic strengthening of intragranular and intergranular occurs in (Al_3BC, CNT)/Al laminated composites via in situ nano-Al_3BC, CNTs, Al_4C_3, and Al_2O_3, respectively. Specifically, strong bonding between Al_3BC and Al

inside of the Al grain's interior with its uniform dispersion, as well as a significant decrease in the dislocation annihilation at GBs due to the CNTs, leads to the significant storage capability of dislocations with increased strain hardening and, consequently, uniform tensile ductility at high flow stresses.

The fabrication of (Al_3BC,CNT)/Al composites includes the high-speed shearing process for breaking CNTs clusters and B agglomerations using a molar ratio of Al/B/CNT = 3/1/1, which uniformly coats the surface of the Al flakes (Figure 1a) and the micro–micro rolling (MMR) process (Figure 1b) [17,18] produces the laminated composites (details of the experimental process are given in the Supplementary Materials). Diffraction peaks of Al_3BC and Al were detected using (Al_3BC,CNT)/Al composites (Figure 2b), while only Al peaks were found in (B,CNT)/Al composites (Figure 2a). The formation of Al_3BC was mostly caused by the reaction Al particles with the B element and the carbon formed due to the decomposition of stearic acid during the fabrication process, as well as subsequent annealing [19]. Indeed, due to the appearance of some areas in which boron and carbon atoms are supersaturated, Al_3BC particles are in situ homogeneously nucleated in a solid state with a limited growth rate. In fact, due to the very low solubility of boron and carbon atoms in Al, especially during solid-state reactions [20,21], the growth processes of Al_3BC particles are soon compromised by the deficiency in carbon and boron atoms; consequently, nanoscale Al_3BC particle are formed. However, the presence of Al_4C_3 effectively contributes to heterogeneously nucleated platelet Al_3BC particles of submicron size via the liquid–solid reaction method [22,23]. For this concept, it should be noted that the characteristic peaks of the Al_4C_3 phase have not been observed in (CNT,B)/Al composite powder due to either very low relative content or a lack of formation.

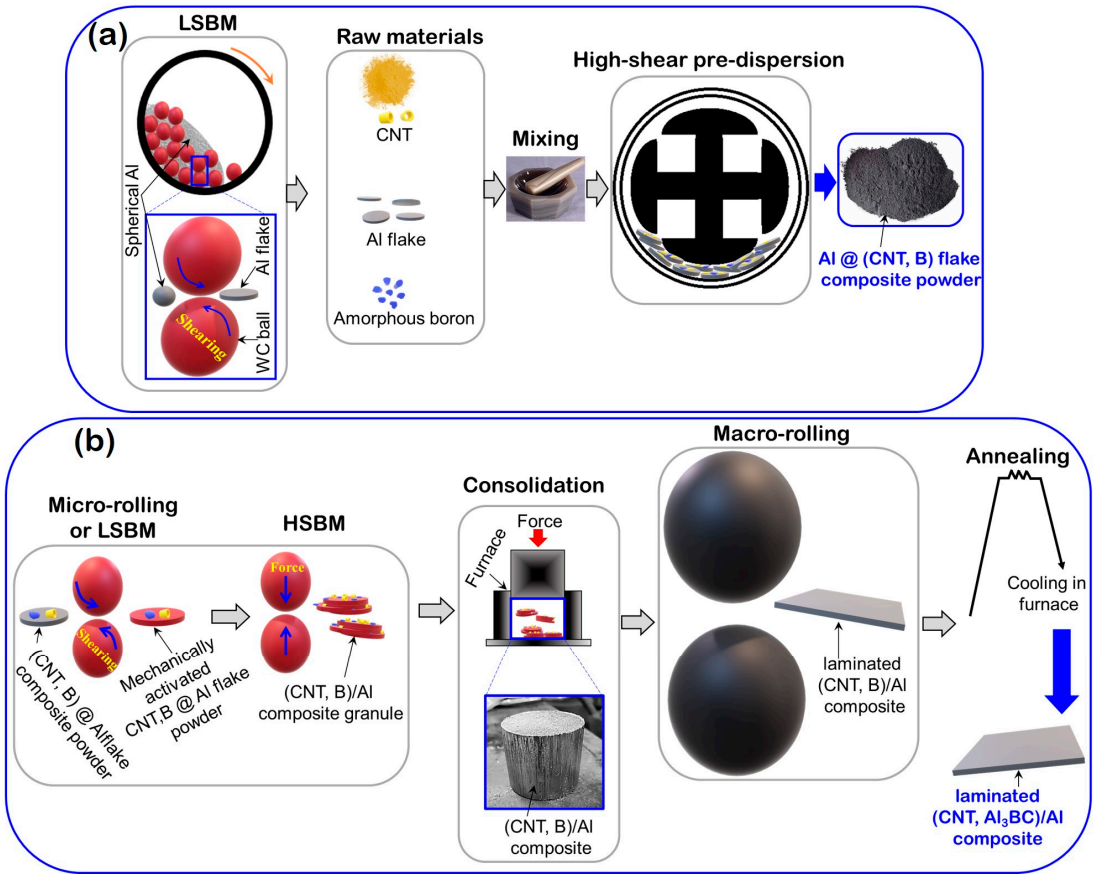

Figure 1. Schematic diagram of (**a**) the preparation of flaky-shape Al/(CNT,B) composite powder and (**b**) the fabrication of laminated (CNT,Al_3BC)/Al composites via the micro–micro rolling (MMR) process [17].

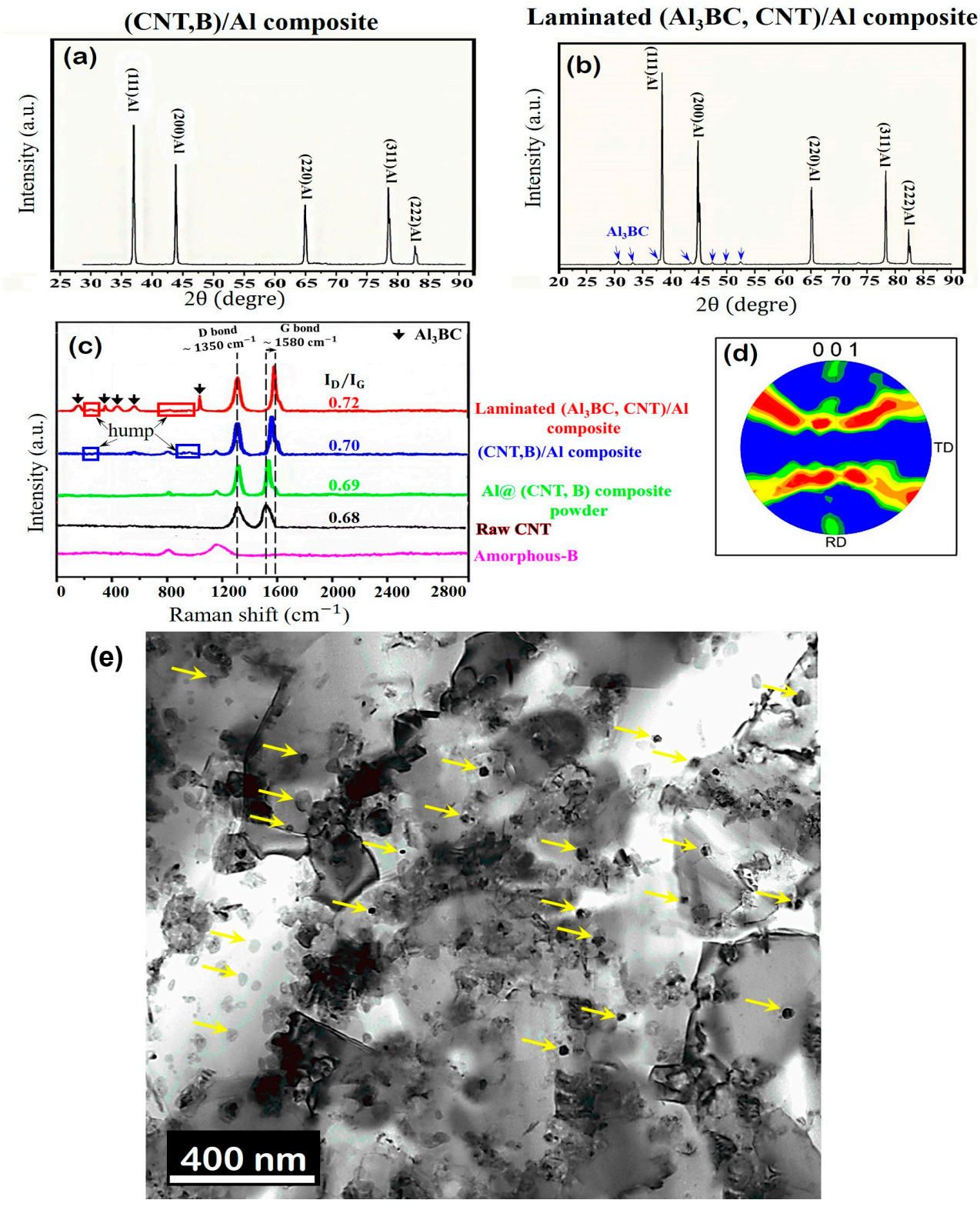

Figure 2. (**a**,**b**) XRD spectra and (**c**) Raman spectra of the studied materials; (**d**) (001) pole figure of a typical (Al_3BC,CNT)/Al laminated composite, (**e**) TEM image of a cross section showing the uniformity of the Al_3BC particle (yellow arrows) dispersion within the UFG Al matrix. (All of the tested sample planes were perpendicular to the RD).

In addition, no specific peak of Al_4C_3 was detected in either the (CNT,B)/Al composite or the (Al_3BC, CNT)/Al laminated composite. This observation is likely due to there being either no reaction between broken CNTs or a low relative content. Comparing the intensities of the peaks, it can be observed that the ratio of {111} intensity to {200} intensity increased after the MMR process, indicating the development of a strong <111> fiber texture. This belief was verified using a typical (001) pole figure, as shown in Figure 2d. As shown in Figure 2c, the relative intensity ratio of the I_D/I_G of the (Al_3BC,CNT)/Al composite increased to 0.72, while the ratio was 0.7, 0.69, and 0.68 for (CNT,B)/Al composite, (CNT,B)/Al composite powder, and raw CNTs, respectively. These results imply that there was almost no serious damage to the CNTs during the pre-dispersion, extrusion, and MMR processes. Additionally, only a peak shift of G-band from ~1580 cm^{-1} to ~1594 cm^{-1} was semi-quantitatively detected in the (Al_3BC, CNT)/Al composite, indicating that it might have originated from the infiltration of Al atoms in CNTs, causing a slight distortion of the sp^2 bonding structures of CNTs. The characteristic peaks of Al_4C_3 [24,25] were not detected in either the (CNT,B)/Al composite or the (Al_3BC,CNT)/Al composite. However, a few sluggish humps appeared in the composites, indicating that slight interface reaction may still exist. Indeed, the formation of Al_4C_3 can result from CNTs that have undergone partial damage, as well as atomic carbon originating from stearic acid when subjected to elevated sintering temperatures. It seems that thanks to the flaky-shaped Al building blocks and the increased available effective surface, the deeper the CNTs are embedded into the Al particles, the smaller the growth value of the I_D/I_G ratio, indicating better protection of the CNTs in both the (CNT,B)/Al composite and the (Al_3BC,CNT)/Al composite [8,26]. Additionally, the TEM image in Figure 2e is provided to demonstrate the distribution of Al_3BC particles within the UFG Al. The criteria used to evaluate uniformity encompassed the absence of localized clustering or agglomeration of Al_3BC particles, ensuring that their distribution was not sporadic but homogeneously spread across the UFG Al. Uniformity was assessed through various characterization techniques, including the TEM image shown in Figure 2e, which, despite its limitations in representing the entire sample, provides a visual indication of the general distribution trend. Furthermore, the uniform distribution of Al_3BC particles contributed to consistent mechanical reinforcement across the composite material. This result occurred because the interactions between dislocations and Al_3BC particles were optimized when particles were evenly distributed, leading to enhanced strengthening effects.

Figure 3a demonstrates an obvious laminated structure with measured grain sizes of approximately 190 and 545 nm. Such an observation is more likely to be associated with the reduced mobility of GB and the subsequent restriction of grain growth caused by the presence of CNTs at the GBs. Furthermore, a significant number of elongated grains exhibited a strong <111> texture, with only a few grains being oriented in the <001> direction. This finding indicates a pronounced restriction of slip, both within the Al grains and at the GBs. The microstructure reveals the presence of a laminated structure with approximately 40% LAGB content. Among these LAGBs, approximately 12% had an angle of $\theta < 3^\circ$, while 28% had an angle of $3^\circ < \theta < 15^\circ$. These LAGBs played a crucial role in strengthening the material through dislocations and the specific strengthening mechanism associated with LAGBs. This outcome is illustrated in Figure 3b. Additionally, approximately 60% of HAGBs were present, most of which were decorated by CNTs, along with some γ-Al_2O_3 nanoparticles. These HAGBs were highly effective in impeding the movement of dislocations, forcing them to tangle and accumulate within the grain interior and near the boundaries. This process resulted in a very high dislocation density of about 1.5×10^{16} m^{-2}, as indicated by the dashed ovals shown in Figure 3c.

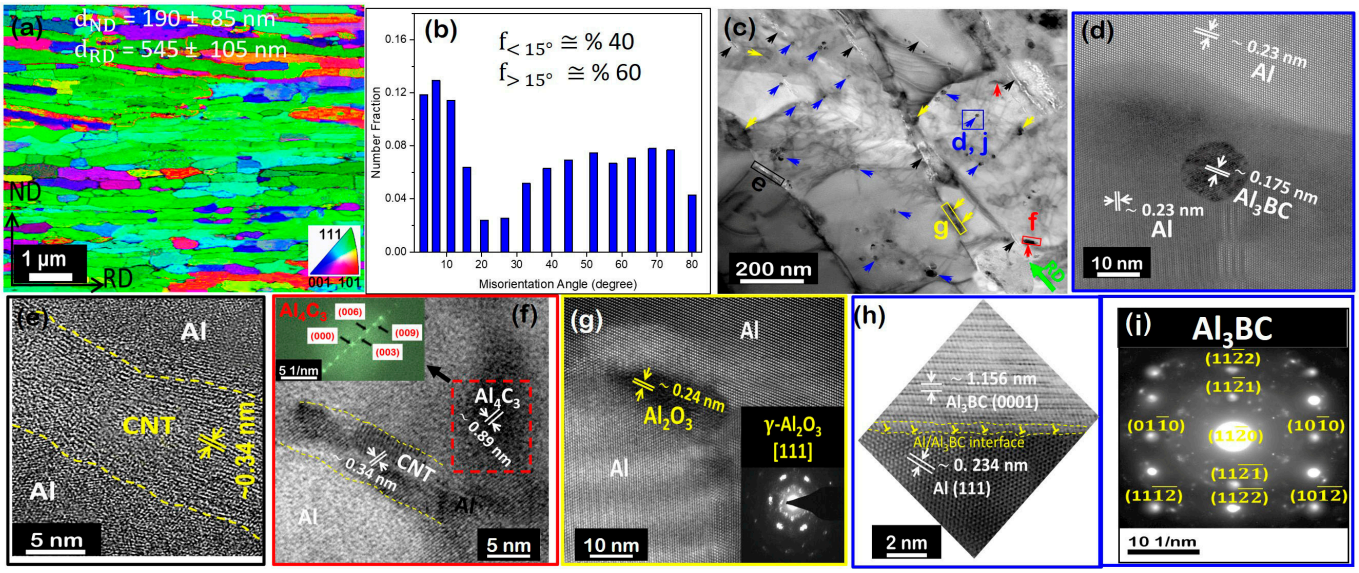

Figure 3. (**a**) EBSD image of (Al_3BC, CNT)/Al laminated composite, (**b**) the distribution of the grain boundary misorientation angle (θ), (**c**) a TEM image showing the elongated Al grains containing different reinforcement elements, (**d**) a STEM image showing a nanoscale Al_3BC in Al matrix, (**e**–**h**), HRTEM images of (**e**) the CNT-Al interface, (**f**) a typical structure of CNTs with small interfacial Al_4C_3, (**g**) the structure of γ-Al_2O_3, (**h**) the Al_3BC–Al interface formed in the grain interior of Al, and (**i**) the relative fast Fourier transforms of Al_3BC. The dashed ovals show dislocation entanglements. The red, black, blue, and yellow arrows show Al_4C_3, CNTs, Al_3BC, and γ-Al_2O_3, respectively.

Upon closer examination of Figure 3c, numerous spherical gray particles in the size range of 15–25 nm can be observed. These particles have been identified as Al_3BC based on the STEM image provided in Figure 3d,j. In thermodynamic terms, it is important to note that Al_3BC has a negative formation enthalpy of approximately −56.34 KJ/mol [27], which is lower than that of Al_4C_3 (~−36 KJ/mol [27]). This observation, coupled with the availability of boron atoms that can form bonds with carbon atoms at damaged CNT tips and the presence of amorphous carbon coating on CNTs, suggests that annealing heat treatment at 800 °C for 3 h in a flowing argon environment would be ideal for the in situ synthesis of Al_3BC nanoparticles. It is expected that the formation of Al_3BC is primarily influenced by the diffusion rate of carbon and boron in the Al matrix. This diffusion rate typically increases in line with temperature in the solid state. Therefore, it is more likely that no Al_3BC would form during hot extrusion, as the high temperature would enhance the diffusion and potentially deplete the available boron atoms. In such a scenario, it is possible that a small number of nanorod-shaped Al_4C_3 particles may form due to exposure to high temperatures when boron atoms become scarce. In other words, the content of Al_4C_3 in this study is not only influenced by temperature, as previously reported by [21], but also strongly depends on the availability of free boron and carbon atoms. The lattice fringes observed in individual Al_3BC, CNT, Al_4C_3, and Al_2O_3 particles in the composites had approximate spacing values of 0.175 nm, 0.34 nm, 0.89 nm, and 0.24 nm, respectively. These spacing values roughly correspond to the (110) plane of Al_3BC, the (1120) plane of graphite, the (003) plane of Al_4C_3, and the (311) plane of γ-Al_2O_3, as shown in Figure 3d–g. In conclusion, nanoscale Al_3BC particles with sizes ranging from 6 to 25 nm have been successfully synthesized in the composites. The size range of the Al_3BC nanoparticles is comparable to those previously synthesized via liquid–solid reaction [23] and self-propagating high-temperature synthesis [28]. In contrast to the complexity and costliness of other proposed routes, the synthesis route proposed in this study is feasible and simple. It involves the direct formation of nanoscale Al_3BC through the reaction between dissolved boron and carbon atoms and the Al matrix, which is achieved through the ball milling, rolling, and annealing processes. The resulting nanorods of in situ Al_4C_3

exhibit strong interfacial bonding, good dispersion within the aluminum grain interior, and a complete single-crystal structure. In the (Al_3BC, CNT)/Al composite, the Al_3BC particles are in situ synthesized and embedded within the Al matrix. The orientation relationship between the Al_3BC particles and the Al matrix is represented by (0111) Al_3BC/(111) Al, which means that the crystallographic planes of Al_3BC align with those of the Al matrix. This alignment allows a better fit between the two materials, resulting in fewer mismatch dislocations at the interface. Thus, the in situ-Al_3BC/Al interface demonstrates a strong bonding effect, which effectively minimizes the presence of mismatch dislocations at the interface (Figure 3h), corroborating the findings reported in previous studies [29,30]. The strong bonding strength, along with the preferred orientation of the elongated Al grains, significantly contributes to the intragranular strengthening effects of Al_3BC on the Al matrix. The majority of CNTs are embedded in the Al matrix and aligned in the RD, indicating a strong and firm bond between the CNTs and the Al matrix. The presence of a clean interface between the CNTs and Al, which lacks any voids or interfacial products (Figure 3e), suggests that both the preservation of the CNT structure and a strong bonding between Al and CNTs occur, which contribute to load transfer and strengthening. However, a small amount of nanoscale rod-like Al_4C_3 is formed in situ through the reaction of partially damaged CNTs with the Al matrix (indicated via the red arrows shown in Figure 3c). The preferential nucleation of interfacial Al_4C_3 at the open edges of the CNTs suggests that these open edges are more reactive than other parts of the CNTs, and these results are consistent with previous studies' findings [31,32]. It appears that the formation of Al_4C_3 could be related to the shortening and breaking of CNTs, which, in turn, increases the number of carbon atoms available to react with Al and B, leading to the production of in situ Al_3BC nanoparticles. The presence of Al_3C_4 in the composite has an effect on the strength and ductility of the product. Al_3C_4 is a special phase with its own mechanical properties that contribute to all composite materials. The presence of Al_3C_4 nanorods can act as an additional reinforcement in the composite. These nanorods may impede dislocation motion and contribute to forest hardening, thus enhancing the strength of the composite. In addition, strong interfacial bonding can be achieved via the formation of an appropriate amount of Al_4C_3, which can promote load transfer and enhance the fracture elongation of the CNT/Al composite. The size of Al_4C_3 is the most important factor affecting the mechanical properties of the composite. In this study, the interfacial bond was improved, while the mean diameters of the short Al_4C_3 rods in composite were as small as ~30–35 nm; therefore, it causes more outstanding elongation (19.7%). As it is a strong combination, it is not easy for microcracks to form and propagate at the interface during plastic deformation. The effect of Al_3C_4 on curing is more complex and needs further analysis and research. However, since Al_4C_3 is a brittle phase, excess Al_4C_3 negatively affects the mechanical properties of the composite.

Additionally, spherical nanoparticles of γ-Al_2O_3 can be observed within both the interior of the Al grains and at the grain boundaries (indicated via yellow arrows, as shown in Figure 3c). These nanoparticles are the result of the transformation of the native amorphous (am)–Al_2O_3 skin that is broken during processing at temperatures above 450 °C [33]. Therefore, the oxygen introduced during the fabrication process predominantly exists in the form of oxides, specifically γ-Al_2O_3. Considering that the native Al_2O_3 skin on the surface of the nanoflakes is approximately 4 nm thick, the volume fraction of Al_2O_3 is estimated to be about 2.6% (8/300 × 100%) of the total volume of the 300-nanometer nanoflake Al powder, which aligns with the value reported in [33]. By assuming that all oxygen present in am–Al_2O_3 is completely transformed into γ-Al_2O_3 after annealing at 800 °C, it is found that the oxygen content also remains virtually unchanged after annealing. The nano-Al_3BC and Al_4C_3 play important roles in generating high effective stress via forest dislocation cutting and Orowan strengthening, while the CNTs and nano-Al_2O_3 effectively provide high back stress via the accumulation and hindering of dislocation annihilation at the interfaces and GBs. Enhanced strength in composites can be achieved through promoted movable dislocation–reinforcement interactions, leading to improved performance based

on the Orowan strengthening phenomenon [34]. The Orowan strengthening occurs a result of the force exerted on a dislocation to bypass particles within the matrix [35]. In this context, Al_3BC nanoparticles are uniformly dispersed throughout the laminated UFG Al grain, with the interparticle spacing estimated to be approximately 170–190 nm, which is close to the particle diameter of about 190 nm. The intragranular Al_3BC nanoparticles and Al_4C_3 in nanorod form could store mobile dislocations in the form of Orowan loops in the internal regions of Al grains during straining, which more effectively provides HDI stress hardening and forest dislocation hardening. This result is consistent with those reported by Liu et al. [35]. This outcome can reduce the ratio of Orowan strengthening to total strengthening. Considering the overall ultimate tensile strength, other strengthening mechanisms come into play. These mechanisms include forest hardening, which arises from dislocation–dislocation interactions that occur due to the relatively higher dislocation density present, and GB strengthening, which results from the presence of UFG Al grains. Both of these factors significantly contribute to the overall enhancement of the strength of material. The presence of nanoparticles (Al_3BC, Al_2O_3) or even Al_4C_3 nanorods causes mechanical incompatibility and promotes dislocation formation (mostly misorientation at less than 3°, which is taken into account as dislocations [36,37]), resulting in stronger dislocation–dislocation interactions and forest dislocation strengthening. Also, during deformation, GBs prevent dislocation movement due to the misorientation of adjacent grains. Higher misorientation causes resistance to movement [38,39]. In addition, UFG Al has a large GB relative to the grain size, resulting in greater resistance to movement and higher stress. Dislocations from LAGBs (approximately 28%) result in a combination of easy sliding and depositing in the Al lamella, resulting in a combination of high elongation while maintaining high tensile strength. This finding is consistent with the literature mentioned above. Indeed, the presence of a high dislocation density, which is estimated to be approximately 8.13×10^{15} m^{-2}, is primarily attributed to the inhomogeneous deformation between the matrix and the reinforcements. This high dislocation density plays a significant role in generating non-directional short-range local stresses, which facilitate dislocation movement. Moreover, it leads to long-range interactions with mobile dislocations, thereby exerting a directional long-range back stress that opposes the applied stress, especially during forward loading (as illustrated in Figure 4).

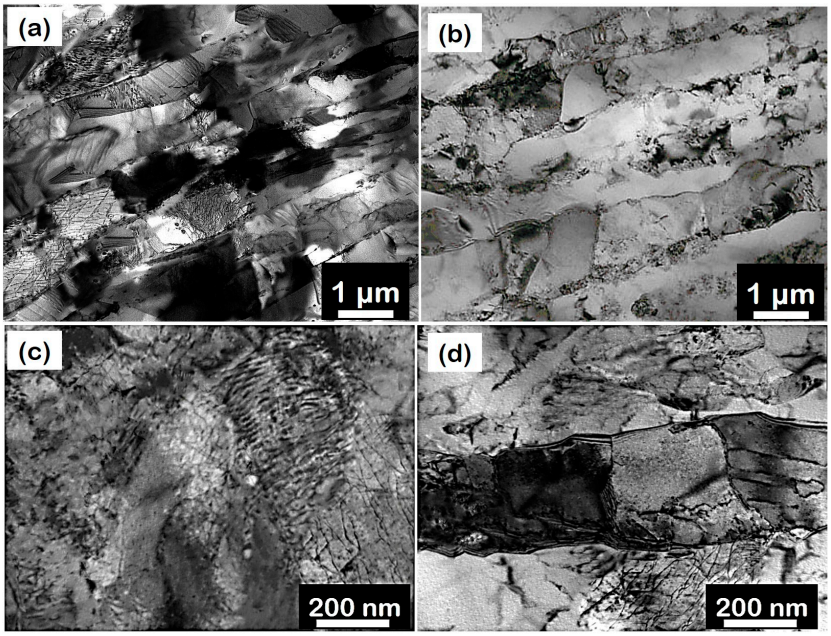

Figure 4. TEM images of (**a**,**c**) (Al_3BC,CNT)/Al and (**b**,**d**) CNT/Al laminated composites showing high density of dislocations.

Figure 5a presents the tensile stress–strain curves of the (Al_3BC,CNT)/Al laminated composites and CNT/Al composites. It is evident that the (Al_3BC,CNT)/Al laminated composites exhibit significantly higher strength than the CNT/Al composites. This result can be attributed to the combined intra- and inter-granular effects of the reinforcements, as well as the laminated structure of the composites. Furthermore, Figure 5b illustrates the variation in the strain-hardening rate as a function of true strain, demonstrating the superior maintenance of a high strain-hardening rate in the (Al_3BC,CNT)/Al laminated composites. The improved dislocation storage capability of ultra-fine-grained (UFG) Al in the (Al_3BC,CNT)/Al laminated composites is attributed to the laminated structure and the in situ formation of intragranular Al_3BC nanoparticles. Specifically, the (Al_3BC,CNT)/Al laminated composites exhibit a strength of 394 MPa, a uniform elongation of 13.2%, and a total elongation of 19.7%, which is approximately 29% higher in strength and shows an increase in the total elongation from 17.7 to 19.5% compared to the CNT/Al composites. Moreover, the uniform elongation of the (Al_3BC,CNT)/Al laminated composites is 13.2%, whereas for PM (powder metallurgy) 16 vol.% B4C/UFG Al with an average grain size of 500 nm, it is only 3.5% [40]. Additionally, for PM (0.5 wt.% CNT, 2 vol.% γ-Al_2O_3)/UFG Al with a unique intragranular dispersion of ultra-short CNTs, the uniform elongation is approximately 5.9% [41]. Considering the similarity of the in situ reinforcements found in the (Al_3BC,CNT)/UFG Al and the 15 vol.% Al_3BC/UFG Al composites [29], the superior strength and ductility of the (Al_3BC,CNT)/UFG Al laminated composite can be attributed to the synergistic contribution of intra- (e.g., in situ formed Al_3BC, partially formed Al_4C_3) and inter-granular strengthening (e.g., CNT, γ-Al_2O_3). The presence of in situ formed nano-dispersoids, particularly the spherical nanoparticles of Al_3BC (Figure 5c), contributes to the synergetic intra- and inter-granular reinforcements within the elongated Al grains. This finding highlights the promising strengthening effects of Al_3BC, which benefits from the strong interface with the matrix. The GBs decorated by CNTs and some γ-Al_2O_3 (~2 wt.%) effectively lose their efficiency through dislocation annihilation, as dislocations nucleate in the neighboring matrix grain near the GBs. This process reduces the magnitude of stress concentration [42] and results in an increase in the critical resolved shear stress due to harder dislocation motion. This finding supports the notion that dislocation multiplication and accumulation, rather than annihilation through recovery, are the governing mechanisms. This result can be attributed to the profound role of in situ reinforcements, which mostly formed a strong interface in the Al grain interior. Recently, a significant high combination of ultimate tensile strength and ductility as a consequence of the presence of CNTs and Al_4C_3, as well as a high dislocation density ($\sim 8.13 \times 10^{15}$ m^{-2}), was demonstrated [43]. Most importantly, these dislocations were mostly caused by inhomogeneous deformation between the matrix and the reinforcements; significantly, both produce the non-directional short-range local stress required for a dislocation to move and dramatically provide long-range interactions via mobile dislocations, exerting a directional long-range back stress opposed to the stress applied in the case of forward loading.

Incorporating both Al_3BC and Al_2O_3 improves the mechanical properties of the composite material. This improvement is mostly achieved through Zener drag, which occurs when dispersed particles are randomly distributed within the material matrix. The effectiveness of Zener drag depends on various factors, such as the nature, geometry, size, spacing, and volume fraction of the particles [44]. In our composite, the presence of these nanoparticles effectively prevents the migration of both HAGBs and LAGBs. As a result, dynamic and static recrystallization is hindered, and grain growth is restrained. This characteristic allows the composite to retain its mechanical properties in advanced Al-based MMCs. The introduction of CNTs and some γ-Al_2O_3 to GBs significantly reduces the dislocation annihilation efficiency, thereby contributing to the occurrence of back stress hardening. On the other hand, reinforcements embedded within the grain interior of Al enhance dislocation blocking and forest hardening, leading to the creation of an advanced approach to achieving ultra-high strengthening and toughening efficiency through intragranlar/intergranular dispersion engineering.

Additionally, the integration of CNTs within the GBs significantly hinders the movement of dislocations across the interface between Al and CNTs [45]. This obstruction of GB motion is more effective when using CNTs due to their elongated nanofiber-shaped structure compared to nearly spherical nature of nanoparticles [46]. The unique morphology of CNTs provides a strong impediment to dislocation movement within the composite. By reinforcing the material, CNTs synergistically enhance its strength through related mechanisms, such as load distribution and dislocation inhibition, while preserving the inherent ductility of the Al matrix.

Therefore, the combined effects of Al_3BC, Al_2O_3, and CNTs contribute significantly to the overall improvement in the strength and ductility of the composite. These materials work together through various mechanisms, including Zener drag, dislocation inhibition, and load distribution, to enhance the mechanical properties of the composite while maintaining the malleability of the Al matrix. This multifaceted enhancement strategy offers possibilities to create advanced materials with superior mechanical performances that make them suitable for a wide range of applications. This advancement represents a progression beyond the work of Jiang et al. [10]. The presence of a well-arranged array of in situ-formed hybrid nanoparticle-rich zones, surrounded by CNT-decorated GBs, synergistically enhances both the strength and ductility of the composite material.

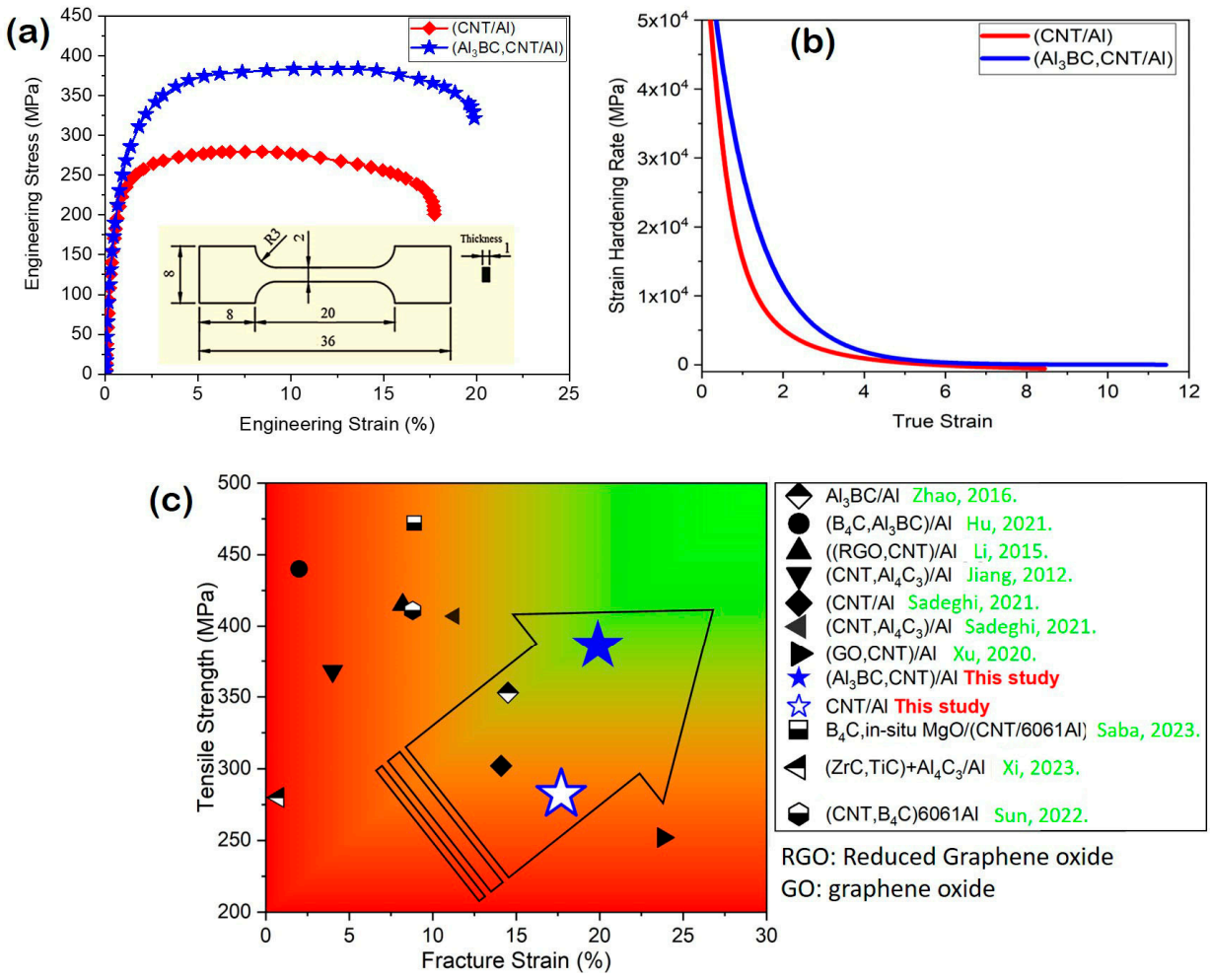

Figure 5. (**a**) Engineering tensile stress–strain curves, (**b**) strain-hardening rate curves of (Al_3BC,CNT/Al) and CNT/Al composites and (**c**) tensile properties of Al composites fabricated via various solid state-based approaches [2,5,27,29,43,47–50]. The arrow shows the direction of the development of the stronger and tougher composites.

Several future directions and potential applications can be explored. Composite materials have a good combination of high strength and ductility, as well as applications in many industries. They are used in lightweight, aerospace, and automotive performance applications to improve fuel efficiency and reduce emissions. In addition, the mechanical properties of composite materials in the medical field facilitate the production of implants and medical devices. To further advance the practical applications of the (Al_3BC, CNT)/Al composite, more research can focus on improving the manufacturing process to develop products using better technology. Exploring the differences and combinations between Al_3BC and CNTs can provide composite materials with unique properties for different applications. Additionally, studying the behavior of composites in different environments, such as high-temperature or corrosive environments, will provide insights into specific applications.

2. Conclusions

In summary, our work presented a new (Al_3BC, CNT)/UFG Al composite sheet that exhibits good support–length properties, having a strength of about 394 MPa and an elongation of about 19.7%. The composite achieved a uniform interparticle/interparticle distribution using a dispersion engineering approach that distinguishes it from most AMCs. The success of this composite could be attributed to the good relationship between the in situ nano-Al_3BC particles in the UFG Al particles and the Al_4C_3 formed at the end of the GB. These materials provided more significant support than conventional CNT/UFG Al composites. Through a careful combination of in situ and ex situ reinforcement techniques, we provided support distribution, leading to the development of dislocation blocks, stress recovery, and forest hardening. This process leads to an increase in the strength and ductility of the composite. The success of our combination and the surprising properties of this unique combination opened up new possibilities for research into and further development of advanced materials with improved equipment and general applications. Overall, the exceptional mechanical properties of this composite make it a promising material for use in various real-world applications. For instance, its high strength and strain-hardening capacity can be advantageous for the development of lightweight and resilient structures for use in aerospace, defense, medical device, and engineering system applications.

Supplementary Materials: The following supporting information can be downloaded at: https://www.mdpi.com/article/10.3390/jcs7080332/s1. References [51–54] are cited in the supplementary materials.

Author Contributions: Methodology: B.S. (Behzad Sadeghi), B.S. (Behzad Sadeghian); Validation: B.S. (Behzad Sadeghi); Investigation: B.S. (Behzad Sadeghi), P.C.; Writing—original draft: B.S. (Behzad Sadeghi), B.S. (Behzad Sadeghian); Writing—review & editing: B.S. (Behzad Sadeghi), P.C.; Formal analysis: P.C.; Supervision: P.C.; Funding acquisition: P.C.; Software: B.S. (Behzad Sadeghian); Data curation: B.S. (Behzad Sadeghian). All authors have read and agreed to the published version of the manuscript.

Funding: This research received no external funding.

Institutional Review Board Statement: Not applicable.

Informed Consent Statement: Not applicable.

Acknowledgments: The authors would like to express their sincere gratitude to Niloofar Ebrahimzadeh Esfahani for her invaluable contributions and support during scientific discussions throughout the course of this study. Her insightful insights and thoughtful discussions greatly enriched the quality of our work. Additionally, the authors extend their heartfelt thanks to Nikzad Sadeghi for his invaluable support in providing innovative ideas and engaging discussions that significantly contributed to the development of this research. Their collaborative input and dedication were instrumental in shaping the direction and outcomes of this study.

Conflicts of Interest: The authors declare that they have no conflict of interest.

Impact Statement: A unique approach involving the incorporation of elemental powder mixture was employed for the first time to create a hybrid nanoreinforcement strategy, resulting in the successful attainment of a remarkable combination of strength and ductility in CNT/Al composites.

References

1. Sadeghi, B.; Cavaliere, P.; Pruncu, C.I.; Balog, M.; Marques de Castro, M.; Chahal, R. Architectural design of advanced Al matrix composites: A review of recent developments. *Crit. Rev. Solid State Mater. Sci.* **2022**, 1–71. [CrossRef]
2. Sun, H.; Saba, F.; Fan, G.; Tan, Z.; Li, Z. Micro/nano-reinforcements in bimodal-grained matrix: A heterostructure strategy for toughening particulate reinforced metal matrix composites. *Scr. Mater.* **2022**, *217*, 114774. [CrossRef]
3. Luo, F.; Jiang, X.; Sun, H.; Mo, D.; Zhang, Y.; Shu, R.; Xue, L. Microstructures, mechanical and thermal properties of diamonds and graphene hybrid reinforced laminated Cu matrix composites by vacuum hot pressing. *Vacuum* **2023**, *207*, 111610. [CrossRef]
4. Xu, Z.Y.; Li, C.J.; Wang, Z.; Fang, D.; Gao, P.; Tao, J.M.; Yi, J.H.; Eckert, J. Balancing the strength and ductility of graphene oxide-carbon nanotube hybrid reinforced Al matrix composites with bimodal grain distribution. *Mater. Sci. Eng. A* **2020**, *796*, 140067. [CrossRef]
5. Li, Z.; Fan, G.; Guo, Q.; Li, Z.; Su, Y.; Zhang, D. Synergistic strengthening effect of graphene-carbon nanotube hybrid structure in Al matrix composites. *Carbon* **2015**, *95*, 419–427. [CrossRef]
6. Chen, L.-Y.; Xu, J.-Q.; Choi, H.; Pozuelo, M.; Ma, X.; Bhowmick, S.; Yang, J.-M.; Mathaudhu, S.; Li, X.-C. Processing and properties of magnesium containing a dense uniform dispersion of nanoparticles. *Nature* **2015**, *528*, 539–543. [CrossRef]
7. Fan, G.; Liu, Q.; Kondo, A.; Naito, M.; Kushimoto, K.; Kano, J.; Tan, Z.; Li, Z. Self-assembly of nanoparticles and flake powders by flake design strategy via dry particle coating. *Powder Technol.* **2023**, *418*, 118294. [CrossRef]
8. Sadeghi, B.; Fan, G.; Tan, Z.; Li, Z.; Kondo, A.; Naito, M. Smart Mechanical Powder Processing for Producing Carbon Nanotube Reinforced Al Matrix Composites. *KONA Powder Part. J.* **2022**, *39*, 2022004. [CrossRef]
9. Ma, L.; Zhang, X.; Pu, B.; Zhao, D.; He, C.; Zhao, N. Achieving the strength-ductility balance of boron nitride nanosheets/Al composite by designing the synergistic transition interface and intragranular reinforcement distribution. *Compos. Part B Eng.* **2022**, *246*, 110243. [CrossRef]
10. Jiang, L.; Yang, H.; Yee, J.K.; Mo, X.; Topping, T.; Lavernia, E.J.; Schoenung, J.M. Toughening of Al matrix nanocomposites via spatial arrays of boron carbide spherical nanoparticles. *Acta Mater.* **2016**, *103*, 128–140. [CrossRef]
11. Zhu, Y.; Wu, X. Heterostructured materials. *Prog. Mater. Sci.* **2023**, *131*, 101019. [CrossRef]
12. Lu, L.; Zhao, H. Progress in Strengthening and Toughening Mechanisms of Heterogeneous Nanostructured Metals. *Acta Metall. Sin.* **2022**, *58*, 1360–1370. [CrossRef]
13. Ma, X.L.; Huang, C.X.; Xu, W.Z.; Zhou, H.; Wu, X.L.; Zhu, Y.T. Strain hardening and ductility in a coarse-grain/nanostructure laminate material. *Scr. Mater.* **2015**, *103*, 57–60. [CrossRef]
14. Pu, B.; Zhang, X.; Chen, X.; Lin, X.; Zhao, D.; Shi, C.; Liu, E.; Sha, J.; He, C.; Zhao, N. Exceptional mechanical properties of Al matrix composites with heterogeneous structure induced by in-situ graphene nanosheet-Cu hybrids. *Compos. Part B Eng.* **2022**, *234*, 109731. [CrossRef]
15. Wan, J.; Yang, J.; Zhou, X.; Chen, B.; Shen, J.; Kondoh, K.; Li, J. Superior tensile properties of graphene/Al composites assisted by in-situ alumina nanoparticles. *Carbon* **2023**, *204*, 447–455. [CrossRef]
16. Zhang, Y.; Li, X. Bioinspired, graphene/Al_2O_3 doubly reinforced Al composites with high strength and toughness. *Nano Lett.* **2017**, *17*, 6907–6915. [CrossRef]
17. Sadeghi, B.; Cavaliere, P.; Balog, M.; Pruncu, C.I.; Shabani, A. Microstructure dependent dislocation density evolution in micro-macro rolled Al_2O_3/Al laminated composite. *Mater. Sci. Eng. A* **2022**, *830*, 142317. [CrossRef]
18. Sadeghi, B.; Cavaliere, P.; Pruncu, C.I. Architecture dependent strengthening mechanisms in graphene/Al heterogeneous lamellar composites. *Mater. Charact.* **2022**, *188*, 111913. [CrossRef]
19. Kleiner, S.; Bertocco, F.; Khalid, F.; Beffort, O. Decomposition of process control agent during mechanical milling and its influence on displacement reactions in the Al–TiO_2 system. *Mater. Chem. Phys.* **2005**, *89*, 362–366. [CrossRef]
20. Dabouz, R.; Bendoumia, M.; Belaid, L.; Azzaz, M. Dissolution of Al 6%wt c Mixture Using Mechanical Alloying. *Defect Diffus. Forum* **2019**, *391*, 82–87. [CrossRef]
21. Kubota, M.; Cizek, P. Synthesis of Al_3BC from mechanically milled and spark plasma sintered Al–MgB_2 composite materials. *J. Alloys Compd.* **2008**, *457*, 209–215. [CrossRef]
22. Zhao, Y.; Ma, X.; Zhao, X.; Chen, H.; Liu, X. Enhanced aging kinetic of Al_3BC/6061 Al composites and its micro-mechanism. *J. Alloys Compd.* **2017**, *726*, 1053–1061. [CrossRef]
23. Zhao, Y.; Qian, Z.; Liu, X. Identification of novel dual-scale Al_3BC particles in Al based composites. *Mater. Des.* **2016**, *93*, 283–290. [CrossRef]
24. Jiang, Y.; Tan, Z.; Fan, G.; Zhang, Z.; Xiong, D.-B.; Guo, Q.; Li, Z.; Zhang, D. Nucleation and growth mechanisms of interfacial carbide in graphene nanosheet/Al composites. *Carbon* **2020**, *161*, 17–24. [CrossRef]
25. Sadeghi, B.; Cavaliere, P. CNTs reinforced Al-based composites produced via modified flake powder metallurgy. *J. Mater. Sci.* **2022**, *57*, 2550–2566. [CrossRef]

26. Wei, H.; Li, Z.Q.; Xiong, D.B.; Tan, Z.Q.; Fan, G.L.; Qin, Z.; Zhang, D. Towards strong and stiff carbon nanotube-reinforced high-strength Al alloy composites through a microlaminated architecture design. *Scr. Mater.* **2014**, *75*, 30–33. [CrossRef]
27. Hu, Q.; Guo, W.; Xiao, P.; Yao, J. First-principles investigation of mechanical, electronic, dynamical, and thermodynamic properties of Al_3BC. *Phys. B Condens. Matter* **2021**, *616*, 413127. [CrossRef]
28. Tsuchida, T.; Kan, T. Synthesis of Al_3BC in air from mechanically activated Al/B/C powder mixtures. *J. Eur. Ceram. Soc.* **1999**, *19*, 1795–1799. [CrossRef]
29. Zhao, Y.; Qian, Z.; Ma, X.; Chen, H.; Gao, T.; Wu, Y.; Liu, X. Unveiling the Semicoherent Interface with Definite Orientation Relationships between Reinforcements and Matrix in Novel Al_3BC/Al Composites. *ACS Appl. Mater. Interfaces* **2016**, *8*, 28194–28201. [CrossRef]
30. Zhao, Y.; Ma, X.; Chen, H.; Zhao, X.; Liu, X. Preferred orientation and interfacial structure in extruded nano-Al_3BC/6061 Al. *Mater. Des.* **2017**, *131*, 23–31. [CrossRef]
31. Chen, B.; Jia, L.; Li, S.; Imai, H.; Takahashi, M.; Kondoh, K. In Situ Synthesized Al_4C_3Nanorods with Excellent Strengthening Effect in Al Matrix Composites. *Adv. Eng. Mater.* **2014**, *16*, 972–975. [CrossRef]
32. Zhou, W.; Yamaguchi, T.; Kikuchi, K.; Nomura, N.; Kawasaki, A. Effectively enhanced load transfer by interfacial reactions in multi-walled carbon nanotube reinforced Al matrix composites. *Acta Mater.* **2017**, *125*, 369–376. [CrossRef]
33. Balog, M.; Krizik, P.; Nosko, M.; Hajovska, Z.; Victoria Castro Riglos, M.; Rajner, W.; Liu, D.-S.; Simancik, F. Forged HITEMAL: Al-based MMCs strengthened with nanometric thick Al_2O_3 skeleton. *Mater. Sci. Eng. A* **2014**, *613*, 82–90. [CrossRef]
34. Li, C.; Mei, Q.; Li, J.; Chen, F.; Ma, Y.; Mei, X. Hall-Petch relations and strengthening of Al-ZnO composites in view of grain size relative to interparticle spacing. *Scr. Mater.* **2018**, *153*, 27–30. [CrossRef]
35. Liu, K.; Su, Y.; Wang, X.; Cai, Y.; Cao, H.; Ouyang, Q.; Zhang, D. Achieving simultaneous enhancement of strength and ductility in Al matrix composites by employing the synergetic strengthening effect of micro- and nano-SiCps. *Compos. Part B Eng.* **2022**, *248*, 110350. [CrossRef]
36. Jiang, J.; Britton, T.B.; Wilkinson, A.J. Measurement of geometrically necessary dislocation density with high resolution electron backscatter diffraction: Effects of detector binning and step size. *Ultramicroscopy* **2013**, *125*, 1–9. [CrossRef]
37. Jiang, J.; Britton, T.B.; Wilkinson, A.J. Evolution of dislocation density distributions in copper during tensile deformation. *Acta Mater.* **2013**, *61*, 7227–7239. [CrossRef]
38. Ma, K.; Liu, Z.Y.; Liu, K.; Chen, X.G.; Xiao, B.L.; Ma, Z.Y. Structure optimization for improving the strength and ductility of heterogeneous carbon nanotube/Al–Cu–Mg composites. *Carbon* **2021**, *178*, 190–201. [CrossRef]
39. Lu, F.; Nie, J.; Ma, X.; Li, Y.; Jiang, Z.; Zhang, Y.; Zhao, Y.; Liu, X. Simultaneously improving the tensile strength and ductility of the AlNp/Al composites by the particle's hierarchical structure with bimodal distribution and nano-network. *Mater. Sci. Eng. A* **2020**, *770*, 138519. [CrossRef]
40. Kai, X.; Li, Z.; Fan, G.; Guo, Q.; Tan, Z.; Zhang, W.; Su, Y.; Lu, W.; Moon, W.-J.; Zhang, D. Strong and ductile particulate reinforced ultrafine-grained metallic composites fabricated by flake powder metallurgy. *Scr. Mater.* **2013**, *68*, 555–558. [CrossRef]
41. Liu, Q.; Fan, G.; Tan, Z.; Guo, Q.; Xiong, D.; Su, Y.; Li, Z.; Zhang, D. Reinforcement with intragranular dispersion of carbon nanotubes in Al matrix composites. *Compos. Part B Eng.* **2021**, *217*, 108915. [CrossRef]
42. Li, Z.; Zhao, L.; Guo, Q.; Li, Z.; Fan, G.; Guo, C.; Zhang, D. Enhanced dislocation obstruction in nanolaminated graphene/Cu composite as revealed by stress relaxation experiments. *Scr. Mater.* **2017**, *131*, 67–71. [CrossRef]
43. Sadeghi, B.; Tan, Z.; Qi, J.; Li, Z.; Min, X.; Yue, Z.; Fan, G. Enhanced mechanical properties of CNT/Al composite through tailoring grain interior/grain boundary affected zones. *Compos. Part B Eng.* **2021**, *223*, 109133. [CrossRef]
44. Huang, K.; Logé, R. *Zener Pinning*; Elsevier: Amsterdam, The Netherlands, 2016.
45. Fu, X.; Xu, R.; Yuan, C.; Tan, Z.; Fan, G.; Ji, G.; Xiong, D.-B.; Guo, Q.; Li, Z.; Zhang, D. Strain Rate Sensitivity and Deformation Mechanism of Carbon Nanotubes Reinforced Al Composites. *Metall. Mater. Trans. A* **2019**, *50*, 3544–3554. [CrossRef]
46. Ma, P.-C.; Siddiqui, N.A.; Marom, G.; Kim, J.-K. Dispersion and functionalization of carbon nanotubes for polymer-based nanocomposites: A review. *Compos. Part A Appl. Sci. Manuf.* **2010**, *41*, 1345–1367. [CrossRef]
47. Jiang, L.; Li, Z.Q.; Fan, G.L.; Cao, L.L.; Zhang, D. Strong and ductile carbon nanotube/Al bulk nanolaminated composites with two-dimensional alignment of carbon nanotubes. *Scr. Mater.* **2012**, *66*, 331–334. [CrossRef]
48. Sadeghi, B.; Qi, J.; Min, X.; Cavaliere, P. Modelling of strain rate dependent dislocation behavior of CNT/Al composites based on grain interior/grain boundary affected zone (GI/GBAZ). *Mater. Sci. Eng. A* **2021**, *820*, 141547. [CrossRef]
49. Saba, F.; Sun, H.; Fan, G.; Tan, Z.; Xiong, D.-B.; Li, Z.; Li, Z. Strength-ductility synergy induced by high-density stacking faults in Al alloy composites with micro/nano hybrid reinforcements. *Compos. Part A Appl. Sci. Manuf.* **2023**, *173*, 107700. [CrossRef]
50. Xi, L.; Feng, L.; Gu, D.; Prashanth, K.G.; Kaban, I.; Wang, R.; Xiong, K.; Sarac, B.; Eckert, J. Microstructure formation and mechanical performance of micro-nanoscale ceramic reinforced Al matrix composites manufactured by laser powder bed fusion. *J. Alloys Compd.* **2023**, *939*, 168803. [CrossRef]
51. He, C.; Zhao, N.; Shi, C.; Song, S. Mechanical properties and microstructures of carbon nanotube-reinforced Al matrix composite fabricated by in situ chemical vapor deposition. *J. Alloys Compd.* **2009**, *487*, 258–262. [CrossRef]
52. Yan, L.P.; Tan, Z.Q.; Ji, G.; Li, Z.Q.; Fan, G.L.; Schryvers, D.; Shan, A.D.; Zhang, D. A quantitative method to characterize the Al4C3-formed interfacial reaction: The case study of MWCNT/Al composites. *Mater. Charact.* **2016**, *112*, 213–218. [CrossRef]

53. Williamson, G.; Smallman, R., III. Dislocation densities in some annealed and cold-worked metals from measurements on the X-ray debye-scherrer spectrum. *Philos. Mag.* **1956**, *1*, 34–46. [CrossRef]
54. Lahiri, D.; Bakshi, S.R.; Keshri, A.K.; Liu, Y.; Agarwal, A. Dual strengthening mechanisms induced by carbon nanotubes in roll bonded aluminum composites. *Mater. Sci. Eng. A* **2009**, *523*, 263–270. [CrossRef]